Received: 12 October 2020 | Revised: 14 December 2020 | Accepted: 30 December 2020

DOI: 10.1111/ijag.15867

INTERNATIONAL JOURNAL OF Applied Glass SCIENCE

ORIGINAL ARTICLE

Fluorine loss determination in bioactive glasses by laser-induced breakdown spectroscopy (LIBS)

Araceli de Pablos-Martín[1,2] | **Altair T. Contreras Jaimes**[2] | **Stefanie Wahl**[3] | **Sylke Meyer**[3] | **Delia S. Brauer**[2]

[1]Fraunhofer Institute for Microstructure of Materials and Systems IMWS, Halle, Germany

[2]Otto Schott Institute of Materials Research, Friedrich Schiller University, Jena, Germany

[3]Fraunhofer Center for Silicon Photovoltaics CSP, Halle, Germany

Correspondence
Dr. Araceli de Pablos-Martín, Otto Schott Institute of Materials Research, Friedrich Schiller University, Fraunhoferstraße 6, 07743 Jena, Germany.

Funding information
Deutsche Forschungsgemeinschaft, Grant/Award Number: BR 4608/7-1 and PA 3095/1-1

Abstract

Fluoride-containing bioactive glasses and glass-ceramics in the SiO_2-P_2O_5-CaO-CaF_2 system are of great interest for dental applications, where the precipitation of fluorapatite supports tooth remineralization. Fluorine quantification in those glasses is key to estimate thermal properties and crystallization tendency. This work presents a study on fluorine determination by laser induced breakdown spectroscopy (LIBS) in four melt-derived glass powders with varying P_2O_5 concentrations. LIBS enables fluorine quantification with a reduced analysis time, minimal to no sample preparation, and high spatial resolution. The fluorine calibration curve was obtained from CaF_2 and SiO_2 mixtures as reference samples, and the fluorine loss upon glass melting has been determined as a function of P_2O_5 content. The P_2O_5-free glass shows the lowest fluorine loss (13%), with HF volatilization likely being responsible for the loss. By contrast, the glass with the highest P_2O_5 content (11.33 wt%) exhibits the largest fluorine loss (55%), owing to additional mechanisms involving the volatilization of phosphorus species like POF_3.

KEYWORDS

bioactive glasses, chemical analysis, fluoride containing glasses, glass melting, LIBS

1 | INTRODUCTION

Chemical analysis is crucial when developing materials since their chemical composition is inherently related to their properties. In many cases, the final composition of a specimen does not correspond with the theoretical (nominal) one, since undesired chemical reactions between raw materials or between raw materials and the environment (decomposition or evaporation during thermal treatments, irradiation, interaction with air, etc.) may occur during processing. In such cases, initial and desired stoichiometry and, potentially, reproducibility and the intended properties of the material may be compromised. Chemical analysis is particularly important in glass science and technology, owing to the high temperatures achieved during the glass melting process (usually above 1000°C), which can lead to evaporation of volatile compounds. Fluoride-containing glasses are especially affected, since fluoride species present high vapor pressures at these melting conditions[1] and, thus, fluorine losses occur during glass melting, typically as either SiF_4 or HF.[2] However, further volatile species present in the glass must be considered as well,[3] for example, the loss as volatile SnF_2 in a stannous fluoro-phosphate glass system.

In the glass industry, fluoride compounds are added as opacifiers of glasses and glass-ceramics. Fluoride-containing glasses present high transparency in the UV to IR spectral

region and low refractive index.[4] Thus, they are of interest for a broad range of optical applications, including telecommunications, optoelectronics, near-infrared or mid-infrared emissions, lenses, and filters. Fluoride-containing bioactive glasses have been studied in great detail as well,[2,5,6] as fluoride plays an important role in the development of biomaterials for dental applications. It inhibits enamel demineralization by forming fluorapatite, which is more acid resistant and has a lower solubility than carbonated hydroxyapatite.[6-9]

Glass-ceramics are prepared by controlled crystallization of the parent glasses. In fluoride-containing glass-ceramics, where fluoride crystals are embedded in the glassy matrix, the retention of fluorine during melting is critical to avoid limitation of the resulting crystalline fraction. Relevant examples of the importance of minimizing fluorine loss in the achieved crystalline fraction are oxyfluoride systems for optical applications[10-13] and bioactive glass-ceramics.[2,8,9] In 1982 Kokubo *et al*.[5,14] developed the commercial bioactive glass-ceramic Cerabone-AW® (Nippon Electric Glass Co, Japan) based on a SiO_2-P_2O_5-CaO-MgO-CaF_2 system. This glass-ceramic consisted of surface crystallized oxyfluorapatite and wollastonite crystals embedded in a glassy matrix. It was shown that this material formed a tight bond to bone and had improved mechanical properties compared to bioactive glasses. Moreover it could be machined into various shapes, which added an important benefit for clinical applications.[15]

Fluorine loss has important consequences for the thermal behavior of glasses.[16] It affects the glass transition temperature (T_g) and influences the crystallization tendency.[2,8,9] Thus, it is necessary to know the actual fluoride content of the glass under investigation and to establish glass preparation protocols, in which the expected fluorine loss during melting is already taken into account when designing new glass compositions. For example, in a study of a fluoro-aluminosilicate glass used for ionomer cement preparation, the fluorine loss was minimized by compositional changes, which allowed for a sufficient number of aluminum ions to bind to fluoride ions, thus decreasing volatilization.[17] In another study[18] the precursor glass and the fluorinating agents (NaF, LiF, MgF_2) were melted separately and then added for a final melting. Moreover, additional quantities of the fluorinating agents were added in the final steps of the melting to balance the loss of fluorides. Fluorine losses in glasses are strongly dependent on the composition. While in bioactive glasses in the system SiO_2-P_2O_5-CaO-CaF_2 fluorine losses are typically in the range between 5 and 23%,[2,19] in oxyfluoride glasses much higher fluorine losses between 30 and 40% have been reported[11,12,20-22]; in the system SiO_2-TiO_2-SrO-SrF_2 even as high as 63%.[23] The use of lids on the crucibles during melting as well as pre-calcined raw materials (decreasing the water content, thereby avoiding the fluoride loss as HF) is highly recommended to increase fluorine retention during melting.[4,12]

Fluorine loss during melting depends strongly on the total fluorine content of the glasses and on the network former/network modifier ratio,[2,4] as well as on the melting temperature and duration of the melting process.[18] Typically, an increase in melting temperature leads to an increase in fluorine evaporation and, thus, to a reduction in the fluoride content in the glasses.[13] The fluorine loss rate in oxyfluoride glasses is reported to be more important in the first minutes of melting (from 5 min at 800°C) and decreases with increasing melting time (until 30 min at 800°C).[16] The nature of the fluorinating agent is also reported to influence fluorine losses.[4]

Several analytical methods are used to determine the fluoride content in materials[17,24,25] (and references therein). A potentiometric method employing a fluoride ion-selective electrode has been used for fluoride quantification in glasses.[16] Here, several dissolution processes including preparation of acidic solutions (HNO_3) and pH adjustments are involved, making this method time consuming. In the particular case of fluoride-containing bioactive glasses, the determination of fluoride release during glass immersion in aqueous solutions is also commonly performed by using a fluoride-selective electrode.[2] In another study,[4] the Ehrlich and Pietzka method[26] was employed. Here, powdered glass samples are mixed with SiO_2 powder and boiled in H_3PO_4. The evaporating SiF_6 is collected in a NaOH solution where the fluoride dissolves and subsequently precipitates as PbBrF. Addition of $AgNO_3$ transforms PbBrF into AgBr, which can be titrimetically quantified through re-titration of $Na_2S_2O_3$ against SCN^- anions. While this method offers a high precision of ±0.01 wt%,[4] it is very complex and labor-intensive. Inductively coupled plasma – optical emission spectroscopy (ICP-OES) is a high-sensitivity atomic spectroscopy technique that is widely available and allows for simultaneous analysis of various elements. However, the fluorine ionization capability is very low in the argon plasma usually employed in this technique,[27] making its detection not feasible.

Electron microscopy-based techniques, like energy-dispersive X-ray spectroscopy (EDXS) are widely used to perform chemical analysis within an SEM microscope, since the sample can be analyzed without complex preparation routes, and usually the EDXS measurement is coupled with the microstructure characterization of the material, obtaining different kinds of information in parallel. However, the analysis of light elements, that is, Be, B, C, N, O, and F, is difficult and not reliable because of their low photon energies (low fluorescence yield), leading to a low signal or low signal/noise ratio. Moreover, low photon energy leads to a high absorption in the specimen and in the detector, resulting in an incorrect measurement of photons and consequently a shift in the peak position. Additionally, low energy peaks are positioned close to the electronic noise of the detection system (which can be seen at about 0 keV). An additional challenge in the fluorine determination by EDXS, especially in glasses,

is the fluoride mobility under the electron beam irradiation,[28] which considerably affects the accuracy of the quantification. However, recent advances in energy-dispersive spectroscopy in combination with the silicon drift detector (SDD) enable an accurate quantification of low atomic number elements, including fluorine.[22,29]

One of the most common methods to quantify the fluorine content in glasses is X-ray fluorescence (XRF) spectroscopy.[30] However, a large error and a high average lower limit of detection of about 1-10 μg/g is associated with XRF.[30] In some cases, a fusion process of the employed pressed powders is needed to homogenize the sample and avoid particle size effects, which would lead to a smaller error. Borate species, like $Li_2B_4O_7$, are used as fusion material and glass-forming agent for XRF analyses.[11,21,30] More recent publications reported on wavelength-dispersive x-ray fluorescence (WD-XRF) spectrometry.[13,25] Here, an electron probe micro analyzer (EPMA) equipped with five wavelength dispersive x-ray analyzers (WDX) was used to determine the fluoride content with an accuracy of ±0.1 at%.[13,19] The measurements were performed at the surface of polished bulk samples, showing that a certain amount of sample preparation is required.

Fluorine can be also determined by quantitative solid-state nuclear magnetic resonance (NMR).[31] However, typical disadvantages are weighing imprecisions, as only about 20-50 mg of sample is used to fill the rotor, and, depending on the probe, the presence of ^{19}F background signals, the suppression of which requires additional measurements. Moreover, a potential systematic error may arise if the relaxation times of the sample and the employed standard differ, the correction of which requires additional measurements, as well.[31]

Laser-induced breakdown spectroscopy (LIBS) is a well-established spectroscopic method for *in situ* elemental analysis, which has the advantage of being minimally destructive.[24,32-35] A short duration high-energy laser pulse is focused on the surface of a sample. Parts of the sample are heated, vaporized, and partly ionized at temperatures up to 10 000°C, and a plasma is generated, where different atomization, ionization, and excitation processes take place (Figure 1A). The radiation emitted by the excited species present in the plasma when the plasma cools down provides chemical information about the sample,[36] and therefore qualitative as well as quantitative analysis is possible, with limits of detection being in the ppm range.[37] One of the major advantages of LIBS in comparison with the above-mentioned methods is the reduced analysis time, minimal to no sample pre-treatment, multi-elemental detection, high spatial resolution and the potential to carry out in-lab, in situ or stand-off (remote, also called TELELIBS[38]) analysis.[39] It has also been shown to offer comparable results to more established analytical techniques such as XRF.[40]

LIBS has been used to quantify fluorine in different materials,[33,39,41] but so far not much information is available on its application for glasses. As the above-mentioned advantages of LIBS have the potential to be very beneficial in the determination of fluorine in bioactive glasses, we decided to investigate its use for this purpose. Here, four bioactive glasses in the system SiO_2-P_2O_5-CaO-CaF_2 with varying P_2O_5 content were prepared by a melt-quench route. CaF_2 was chosen as fluorinating agent. Fluorine loss is discussed as a function of P_2O_5 content. This work demonstrates that fluorine in melt-derived glasses can be quantified by LIBS, and that this method is useful for studying and, thus, improving the retention of fluorine during melting.

2 | EXPERIMENTAL

2.1 | Sample preparation

Glasses in the system SiO_2-P_2O_5-CaO-CaF_2 were prepared by a melt-quench route. Four glasses were designed based on the network connectivity (NC) model. NC is the average number of bridging oxygens (BO) per network forming element (here silicon, NC_{Si}) in the glass structure.[6,42] In the case of bioactive glasses, Edén *et al.*[43] suggested an NC between 2.0 and 2.6 for optimum bioactivity, with NC = 2.4 being considered in some studies as the cut-off value for bioactivity as defined by Hill.[44] It has been reported that when adding P_2O_5 together with stoichiometric amounts of network modifiers (and thus, keeping NC constant) the bioactivity increases with the phosphate content.[6,42,45] Therefore, in the present work, the P_2O_5 content was varied between 0 and 5.1 mol % while keeping the network connectivity (NC)

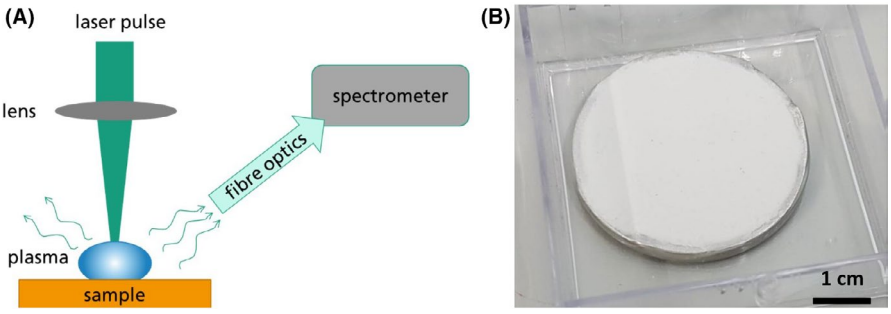

FIGURE 1 (A) Scheme of the principle of operation of LIBS analysis and (B) one of the pressed glass powder compacts with a diameter of ~4 cm used for LIBS analysis

constant at 2.11. Considering a maximum of four bridging oxygen atoms per silicon atom, phosphorus only present as orthophosphate species (PO_4^{3-})[6] and fluoride ions complexing calcium,[46,47] the NC of the studied glasses is calculated according to Equation (1),

$$NC_{Si} = \frac{4\left[SiO_2\right] - 2\left[CaO\right] + 6\left[P_2O_5\right]}{\left[SiO_2\right]} \quad (1)$$

where $[SiO_2]$, $[P_2O_5]$, and [CaO] refer to the molar percentages of each component.[42] As P_2O_5 was added, CaO content was increased simultaneously to provide Ca^{2+} cations for charge balancing the orthophosphate units.

Table 1 shows the nominal compositions of the glasses P0 (phosphate-free), P2, P3 to P5 (with the highest phosphate content).

Glasses were melted in platinum-rhodium crucibles from 150 g batches containing mixtures of the following analytical grade raw materials: SiO_2 (99.0% Carl Roth, Germany), $Ca(H_2PO_4)_2 \bullet 2H_2O$ (Chemische Fabrik Budenheim KG, Germany), CaF_2 (Chemiewerk Nünchritz, Germany), and $CaCO_3$ (≥99.0% Merck, Germany). These raw materials were melted in air in an induction-heated furnace (in-house built). Crucibles were covered with lids. Melting temperatures and times were between 1400 and 1480°C and between 75 and 85 min, respectively, depending on the composition (Table 1). The mixed raw materials were added to the crucible inside the furnace in small additions to reduce foaming. Glasses were cast into a brass mold, pressed with a carbon stamp and annealed at 670 +/- 5 °C for times between 0.5 and 4 hours. Glasses were ground in a metallic mortar and sieved to obtain a particle size range <125 μm. Glass powders were stored in a desiccator until used for further analysis.

2.2 | Reference samples

Reference samples are needed to develop a fluorine calibration curve for the LIBS analysis. Seven reference samples (20 g of each) were prepared by mixing CaF_2 (99.0%, 325 Mesh Powder (45 μm), Alfa Aesar, Germany) and SiO_2 (99.0%, <125 μm, Carl Roth, Germany) according to the weight percentages shown in Table 2. These reagents were manually mixed and further homogenized in a rotatory mixer for 1 day.

2.3 | LIBS analysis

Glass samples (Table 1) as well as the reference samples (Table 2) were pressed with a hydraulic press at a force of 50 kN (TP60, Herzog Maschinenfabrik GmbH) to form powder compacts with a diameter of ~4 cm (Figure 1B).

Since the glass powder samples were collected from the entire volume of the bulk piece of the glasses, it is assumed that the analyzed powder samples are reasonably representative of the total volume of the glasses. Additionally, it has been reported that the particle size influences the LIBS signal; however, without any significant relationship or clear correlation.[48] In fact, the authors in ref.[48] did not observe a significant correlation between statistical particle size distribution and LIBS signal intensity. According to a recent study published in ref.[33] the particle size did not significantly affect fluorine quantification. It also confirmed that fluorine quantification using LIBS is possible without dependence on the particle size if all the samples have roughly the same particle size distribution.

The LIBS experimental set-up used in this work is based on a Nd:YAG laser (FiberLIBS, SECOPTA analytics GmbH) at 1064 nm. Excitation was performed with an energy of 1 mJ per pulse, a pulse duration tp <2 ns and a diameter of the illuminated area of <100 μm. The shot repetition rate was selected as 1000 Hz. The laser distance sensor to determine the focus height works with a semiconductor laser with a wavelength of 635 nm and a performance of 1 W.

The laser head was moved using motorized X–Y micro-translation stages, while the sample can be fixed in a sample holder system. Samples were irradiated in a pattern of 10 x 10 points, with a separation of 0.5 mm. At each point,

TABLE 1 Nominal compositions of the glasses and fluorine content in wt%

	SiO_2		P_2O_5		CaO		CaF_2		F	
Glass	wt%	mol %	wt%	mol %	wt%	mol %	wt%	mol %	wt%	Melting conditions
P0	46.92	46.8	0.00	0	41.36	44.2	11.72	9	5.70	1400°C 75 min
P2	40.74	41.9	5.51	2.4	42.38	46.7	11.37	9	5.53	1480°C 80 min
P3	38.31	39.9	7.71	3.4	42.75	47.7	11.23	9	5.46	1400°C 75 min
P5	34.14	36.3	11.33	5.1	43.53	49.6	11.00	9	5.35	1470°C 85 min

TABLE 2 Compositions (wt%) of the SiO_2-CaF_2 mixtures used as references for the fluorine calibration curve

Relative amount (wt%)	R1	R2	R3	R4	R5	R6	R7
CaF_2	1.00	2.00	4.00	6.00	8.00	10.00	12.00
SiO_2	99.00	98.00	96.00	94.00	92.00	80.00	88.00
F	0.49	0.97	1.95	2.92	3.89	4.87	5.84

a LIBS spectrum is obtained by accumulating 25 single shot emission spectra. Data treatment was carried out using the SEC analysis tool (SECOPTA analytics GmbH). The standard deviation (SD) is given as a measure of the data distribution in relation to the mean value.

For the development of the fluorine calibration curve 100 single spectra per sample (R1 to R7, Table 2) were averaged. The resulting reference spectra of R1 to R7 were used for evaluation. The calibration curve was obtained by the partial least squares (PLS) method included in the SEC analysis tool.

3 | RESULTS AND DISCUSSION

3.1 | Results for reference samples and calibration

Figure 2A displays the LIBS emission spectra of the reference samples. Emission peaks corresponding to Ca (315.9, 317.9, 373.7, 393.4, and 396.8 nm), Si (251.6 and 288.2 nm), and F (685.6 and 690.2 nm) of the references (R1 to R7, Table 2) are observed.

The fluorine emission lines in the spectral range between 680 and 700 nm were used for analysis. Figure 2B shows the fluorine signals of the references (Table 2) centered at 685.6 and 690.2 nm. Considering the LIBS spectra in the range between 680 and 700 nm (Figure 2B), the fluorine calibration curve was calculated (shown in the supplementary material, Figure S1). The spectra were smoothed each by five-point averaging. Normalization was performed relative to the background at 681 nm. With these settings, a coefficient of determination of $R^2 = 0.9896$ and a root mean square error (RMSE) of 0.1887 was obtained. Cross validation was used to verify the method. The coefficient of determination for the cross validation was determined as $R^2 = 0.9608$ and RMSE = 0.3856. The calibrated fluorine concentrations were in the range between 0.5 and 5.8 wt% to cover the concentration range of the analyzed glasses (Table 1).

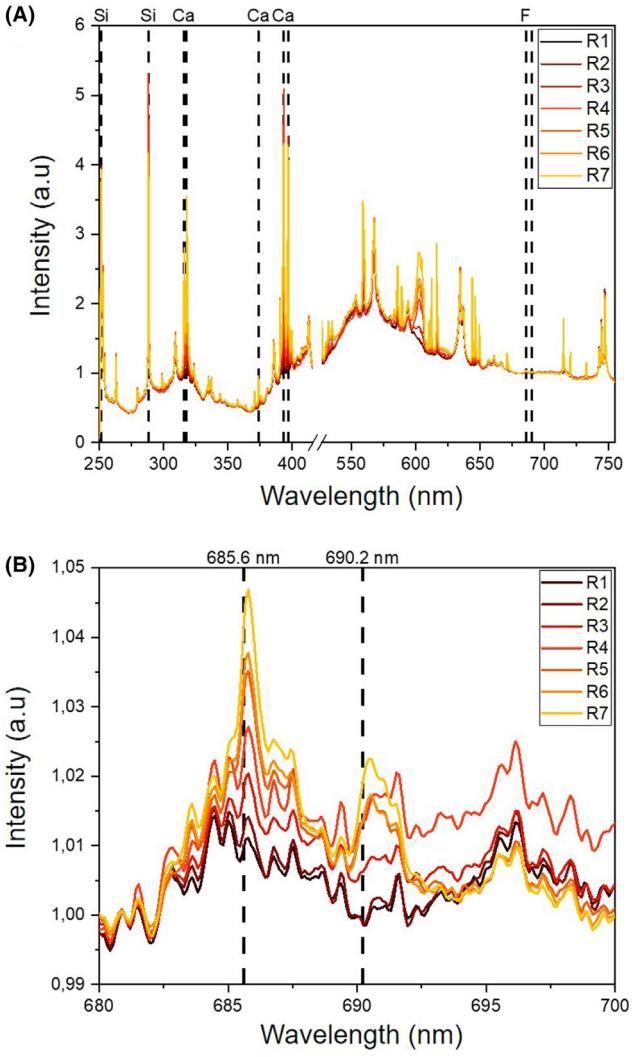

FIGURE 2 (A) LIBS emission spectra of the reference samples (R1-R7) over the full spectral range. Black lines indicate the emission lines of silicon, calcium, and fluorine. (B) LIBS emission spectra of the reference samples (R1-R7) focusing on the fluorine peaks. Black bars indicate the fluorine emission lines

3.2 | Results for glass samples

Spectra of four different glass samples were recorded under the same conditions as the calibration samples. Figure 3A shows the LIBS spectra over the full range. There are some truncated peaks, especially for Ca, owing to an intensity overload of the detector for these wavelengths. Nevertheless, quantification of fluorine (Figure 3B) could be performed if 25 spectra were accumulated, in order to get enough signal intensity of the peaks for quantification.

Table 3 displays the analyzed fluoride concentration (wt%) of the glass samples in comparison with the nominal

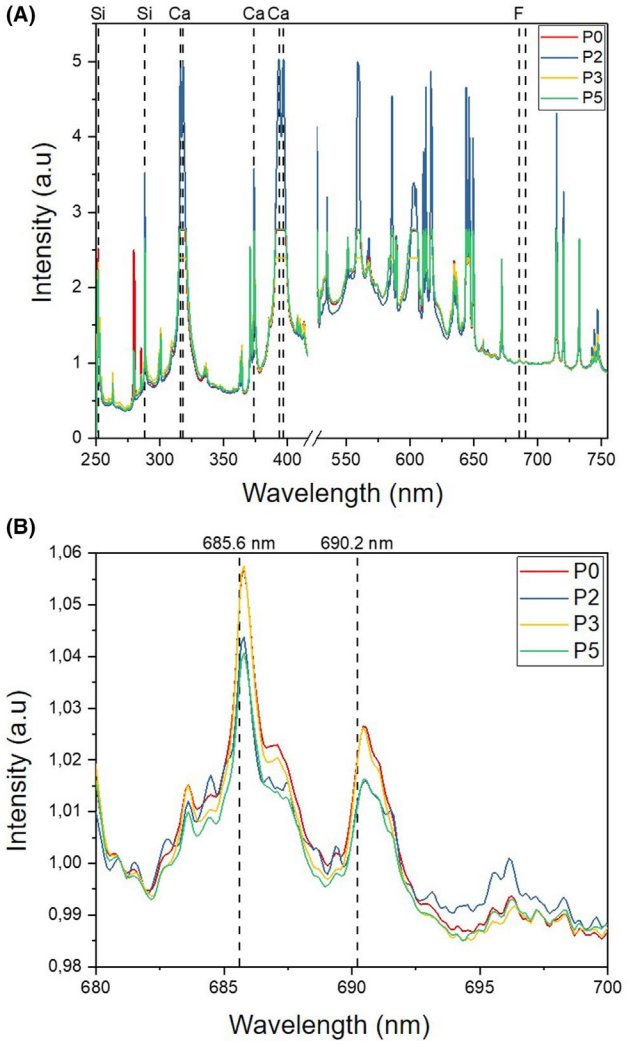

FIGURE 3 (A) LIBS emission spectra of the glass samples P0, P2, P3 and P5 over the full spectral range. There are truncated peaks owing to intensity overload for some wavelengths during the measurement. (B) LIBS spectra of the glass samples P0, P2, P3, and P5 focusing on the fluorine peaks

ones. The fluorine loss associated with the glass melting process was calculated and is shown in Table 3, as well. Fluorine losses are between 13 and 55%, with the phosphate-free glass P0 being the one with the lowest fluorine loss (around 13%) and P5 (highest phosphate content) the one with the highest fluorine loss (around 55%; Table 3). The intermediate glasses P2 and P3 present intermediate fluorine losses. Focusing on glasses of a similar system (SiO_2-P_2O_5-CaO-CaF_2), Brauer *et al.*[2] reported losses between 5 and 23% in glasses in the system SiO_2-P_2O_5-CaO-Na_2O-CaF_2. However, those glasses were melted for 1 h at 1430°C, which is lower than the melting temperatures in the present work (Table 1). In ref.[19] fluorine losses in SiO_2-free glasses in the system P_2O_5-CaO-Na_2O-CaF_2 were determined by EPMA and with a fluoride ion probe, giving 18% and ~21% fluorine loss, respectively. However, in that work, melting conditions were softer, with 950°C for a duration as short as 5 min.

TABLE 3 Nominal and analyzed fluoride concentration including standard deviation (SD) in glass samples P0 to P5 and calculated fluorine loss (%)

Glass	Nominal F concentration (wt%)	LIBSmean F concentration and SD (wt%)	Fluorine loss (%)
P0	5.70	4.96 (1.02)	12.98
P2	5.53	3.20 (1.43)	42.13
P3	5.46	4.02 (1.16)	26.37
P5	5.35	2.42 (1.07)	54.77

Möncke *et al.*[31] reported losses below 15% in $NaPO_3$-AlF glasses. In ref.[13] fluorine losses from 15% to 21% were reported when the melting temperature of Er^{3+}-doped 75$NaPO_3$-25CaF_2 glasses increased from 900°C to 1000°C. Xu *et al.*[49] reported fluorine losses above 50% based on XPS analysis of stannous fluorophosphate glasses doped with PbO and B_2O_3 [93], exposed to a maximum temperature of 500 °C; and around 20% in fluorophosphate glasses based on NMR analysis.[50,51]

The nominal CaF_2 contents of the glasses in the present study (Table 1) were very similar (F content slightly varying between 5.35 and 5.70 wt%), as the glasses differ mostly in their SiO_2 and, most importantly, in their P_2O_5 content. Moreover, the melting conditions were similar as well. Thus, the large differences in fluorine losses between glasses P0 and P5 are most likely to be connected to the P_2O_5 content.

Ehrt[52] reported that phosphate-rich glasses show very high fluorine loss, in contrast to fluoride-rich glasses with low fluorine loss; and that fluorine loss decreased with decreasing phosphate content. Different mechanisms for fluorine losses exist for melt-derived glasses as extensively discussed by Semrau.[53] Traditionally, it was assumed that fluoride ions replace oxygen ions in silicate glasses, thereby forming Si-F bonds and leading to SiF_4 volatilization. However, this mechanism has been proven not to be the main responsible for fluorine loss during glass melting,[53] as silicon ions have a higher affinity for oxygen ions than for fluoride ions, SiF_4 formation would be only plausible in highly cross-linked glasses or high fluoride concentrations. Nevertheless, it has been widely shown that in bioactive glasses, fluoride complexes modifier cations (Ca^{2+}, Na^+ etc.) exclusively, and does not form Si-F bonds, as confirmed by ^{19}F- and ^{29}Si MAS NMR spectroscopy and molecular dynamics simulations.[6,19,46,47,54,55] Thus, fluorine loss in the present glasses is more likely to occur *via* formation of HF from the reaction of water vapor with metal fluorides (CaF_2 in our case) at high temperatures, as illustrated by the following reactions[53]:

$$CaF_2 + H_2O \rightarrow CaO + 2HF \quad (2)$$

$$CaF_2 + H_2O + SiO_2 \rightarrow CaSiO_3 + 2HF \quad (3)$$

This mechanism depends strongly on the water content (both as H_2O and OH^-) of the raw materials used.[4] Brauer *et al.*[2] reported on glasses in the very similar system SiO_2-P_2O_5-Na_2O-CaO-CaF_2 with varying CaF_2 concentration, showing a water loss on ignition at 500 °C between 0.8 and 2.1%, decreasing with increasing CaF_2 content. The decrease of water loss on ignition with increasing CaF_2 content suggests that CaF_2 in the glass impedes absorption of atmospheric water. In that reference, relative fluorine loss did not show any correlation with CaF_2 content, and it was thus assumed to be dependent on atmospheric humidity levels during melting, indicating fluorine evaporation as HF rather than as SiF_4. From all the above-mentioned, fluorine loss in the P_2O_5-free glass P0 is likely to occur through HF volatilization following Eqs. 2 and 3.[53]

Phosphate glasses (P2-P5) can undergo an additional fluoride loss mechanism through POF_3 evaporation[4,53,56]:

$$3CaF_2 + 4P_2O_5 \rightarrow 2POF_3 + 3Ca(PO_3)_2 \quad (4)$$

Hydrolysis of POF_3 leads to the formation of HF as well:

$$POF_3 + H_2O \rightarrow HPO_2F_2 + HF \quad (5)$$

Möncke *et al.*[4] reported that P-F bonds could only be detected in (Na_2O-Al_2O_3-P_2O_5-F) (NAPF) glasses prepared at melting temperatures up to 850°C. P-F bonds were no longer detectable when the glasses where melted near 1000°C. P-F bonds were not detected in ref.[50] on fluorophosphate glasses melted at 1150°C for 5 min either, in good agreement with Eqs. 4 and 5. According to Brauer *et al.*[46] orthophosphate groups are charge-balanced by cations (Ca^{2+} in our glasses) and by Ca-F complexes, which agrees with the chemical reaction in Eq. 4. Thus, P_2O_5-containing glasses undergo fluorine loss *via* POF_3 in addition to HF evaporation mechanisms (Eqs. 2 and 3), explaining a higher fluorine loss in the P-containing glass P5 in comparison with the P-free glass P0 (Table 3). A combination of these reactions is likely to occur in the intermediate P2 and P3 glasses. However, a change of the trend in the P3 glass is observed (Table 3), which may be explained by a slightly lower melting temperature and shorter time in the P3 glass (Table 1) in comparison with those of P2 and P5 glasses (fluorine loss has been reported to be critical in the first minutes of the melting and decreases at longer periods[16,19]), or even by a heterogeneous distribution of the powdered sample.

Another parameter that may influence fluorine loss is the viscosity of the glass melts. In general, viscosity increases with increasing phosphate content and decreases with fluorine concentration.[57] In ref.[58] viscosity-temperature curves of the most common bioactive glasses were reported.

4 | CONCLUSIONS

Fluorine loss during the melting of bioactive glasses in the system SiO_2-P_2O_5-CaO-CaF_2 system with varying P_2O_5 concentrations has been quantified using the LIBS method. LIBS analysis offers a reduced analysis time and minimal sample preparation. Results suggest that with increasing phosphate concentrations in the glass more fluorine was lost during melting. While silicate glasses typically lose fluorine as HF, in phosphate-containing silicate glasses additional mechanisms of fluoride loss exist, in which the volatilization as POF_3 takes place. Thus, although the network connectivity was the same in all the investigated glasses, P_2O_5 strongly influenced fluoride retention in the glass melt. While both fluorine and phosphate have been shown to have various beneficial effects on bioactive glass properties, our results suggest that fluorine loss measurements need to be performed to ensure a proper evaluation of the composition-properties relationship of the glasses.

Improving the melting conditions to minimize fluorine losses is key. The preparation of glasses in the studied system at lower melting temperatures and shorter melting times (to reduce the fluoride loss, while ensuring a homogeneous melt) is part of a future work. Fluorine losses of those glasses will be compared to the ones reported in the present study, to investigate the influence of the melting conditions on fluoride retention. The structural characterization of the investigated glasses is part of a forthcoming publication, which will provide the relationship between atomic structure and fluorine loss.

ACKNOWLEDGEMENTS

The authors thank Angelika Hacker (Otto Schott Institute) for assistance with the preparation of standard mixtures, Gloria Kirste for glass preparation and the German Research Foundation (DFG) for providing funding to carry out the project (grant numbers BR 4608/7-1 and PA 3095/1-1).

ORCID

Araceli de Pablos-Martín https://orcid.org/0000-0002-9824-6273
Delia S. Brauer https://orcid.org/0000-0001-5062-0695

REFERENCES

1. Parker JM, West GF. Model study of SiF_4 volatilisation from an oxide glass melt. Mater Sci Forum. 1986;7:297–306.
2. Brauer DS, Mneimne M, Hill RG. Fluoride-containing bioactive glasses: fluoride loss during melting and ion release in tris buffer solution. J Non-Cryst Solids. 2011;357(18):3328–33.
3. Wang YJ, Yu Y, Zou Y, Zhang LY, Hu LL, Chen DP. Broadband visible luminescence in tin fluorophosphate glasses with ultra-low glass transition temperature. RSC Adv. 2018;8(9):4921–7.

4. Möncke D, Neto MCB, Bradtmüller H, de Souza GB, Rodrigues AM, Elkholy HS, et al. $NaPO_3$-AlF_3 glasses: fluorine evaporation during melting and the resulting variations in structure and properties. J Chem Technol Metall. 2018;53(6):1047–60.
5. Duminis T, Shahid S, Hill RG. Apatite glass-ceramics: a review. Adv Mater Res. 2017;3:1–15.
6. Brauer DS. Bioactive glasses - structure and properties. Angew Chem Int Edit. 2015;54(14):4160–81.
7. Donald IW. The science and technology of inorganic glasses and glass-ceramics: from the ancient to the present to the future. Chapeltown, Sheffield: Society of Glass Technology; 2016.
8. Brauer DS, Anjum MN, Mneimne M, Wilson RM, Doweidar H, Hill RG. Fluoride-containing bioactive glass-ceramics. J Non-Cryst Solids. 2012;358(12):1438–42.
9. Brauer DS, Hill RG, O'Donnell MD. Crystallisation of fluoride-containing bioactive glasses. Eur J Glass Sci Technol B-Phys Chem Glasses. 2012;53(2):27–30.
10. De Pablos-Martín A, Durán A, Pascual MJ. Nanocrystallisation in oxyfluoride systems: mechanisms of crystallisation and photonic properties. Int Mater Rev. 2012;57:165–86.
11. De Pablos-Martín A, Ristic D, Bhattacharyya S, Höche T, Mather GC, Ramírez MO, et al. Effects of Tm^{3+} additions on the crystallization of LaF_3 nanocrystals in oxyfluoride glasses: Optical characterization and up-conversion. J Am Ceram Soc. 2013;96(2).
12. Hémono N, Pierre G, Muñoz F, de Pablos-Martín A, Pascual MJ, Durán A. Processing of transparent glass-ceramics by nanocrystallisation of LaF_3. J Eur Ceram Soc. 2009;29:2915–20.
13. Szczodra A, Mardoukhi A, Hokka M, Boetti NG, Petit L. Fluorine losses in Er^{3+}oxyfluoride phosphate glasses and glass-ceramics. J Alloy Compd. 2019;797:797–803.
14. Kokubo T, Shigematsu M, Nagashima Y, Tashiro M, Nakamura T, Yamamuro T, et al. Apatite- and wollastonite-containg glass-ceramics for prosthetic application. Bull Inst Chem Res Kyoto Univ. 1982;60.
15. Duminis T, Shahid S, Hill RG. Apatite glass-ceramics: a review. Front Mater. 2017;3.
16. Bueno LA, Messaddeq Y, Dias Filho FA, Ribeiro SJL. Study of fluorine losses in oxyfluoride glasses. J Non-Cryst Solids. 2005;351(52):3804–8.
17. Hurrell-Gillingham K, Reaney IM, Miller CA, Crawford A, Hatton PV. Devitrification of ionomer glass and its effect on the in vitro biocompatibility of glass-ionomer cements. Biomaterials. 2003;24(18):3153–60.
18. Kalo H, Möller MW, Ziadeh M, Dolejš D, Breu J. Large scale melt synthesis in an open crucible of Na-fluorohectorite with superb charge homogeneity and particle size. Appl Clay Sci. 2010;48(1):39–45.
19. Nommeots-Nomm A, Houaoui A, Pradeepan Packiyanathar A, Chen X, Hokka M, Hill R, et al. Phosphate/oxyfluorophosphate glass crystallization and its impact on dissolution and cytotoxicity. Mater Sci Eng C. 2020;117:111269.
20. Bocker C, Muñoz F, Durán A, Rüssel C. Fluorine sites in glasses and transparent glass-ceramics of the system $Na_2O/K_2O/Al_2O_3/SiO_2/BaF_2$. J Solid State Chem. 2011;184(2):405–10.
21. de Pablos-Martín A, Mather GC, Muñoz F, Bhattacharyya S, Höche TH, Jinschek JR, et al. Design of oxy-fluoride glass-ceramics containing $NaLaF_4$ nano-crystals. J Non-Cryst Solids. 2010;356:3071–9.
22. Stoica M, Brehl M, Bocker C, Herrmann A, Rüssel C. Microstructure and luminescence of erbiumdoped $Na_2O/K_2O/CaO/CaF_2/Al_2O_3/SiO_2$ nano glass-ceramics. Mater Chem Phys. 2018;207:36–43.
23. Hong L, Qing Y, Ning H. Influence of fluorine on the structure and luminescence properties of Sm^{3+} doped strontium titanium silica glass. Key Eng Mat. 2012;509:273–8.
24. Carter S, Clough R, Fisher A, Gibson B, Russell B, Waack J. Atomic spectrometry update: review of advances in the analysis of metals, chemicals and materials. J Anal Atom Spectrom. 2019;34(11):2159–216.
25. Gazulla MF, Rodrigo M, Orduña M, Ventura MJ. Fluorine determination in glasses and glazes by WD-XRF. Eur J Glass Sci Technol A-Glass Technology. 2015;56(3):95–101.
26. Ehrlich P, Pietzka G. Die maßanalytische Bestimmung des Fluors nach Fällung als Bleibromofluorid. Fresenius' Zeitschrift für analytische Chemie. 1951;133(1):84–94.
27. Mello PA, Barin JS, Duarte FA, Bizzi CA, Diehl LO, Muller EI, et al. Analytical methods for the determination of halogens in bioanalytical sciences: a review. Anal Bioanal Chem. 2013;405(24):7615–42.
28. de Pablos-Martin A, Patzig C, Hohe T, Duran A, Pascual MJ. Distribution of thulium in Tm^{3+}-doped oxyfluoride glasses and glass-ceramics. CrystEngComm. 2013;15(35):6979–85.
29. Newbury DE, Ritchie NWM. Performing elemental microanalysis with high accuracy and high precision by scanning electron microscopy/silicon drift detector energy-dispersive X-ray spectrometry (SEM/SDD-EDS). J Mater Sci. 2015;50(2):493–518.
30. Schramm R. Use of X-ray fluorescence analysis for the determination of rare earth elements. Phys Sci Rev. 2016;1(9):20160061.
31. Möncke D, Eckert H. Review on the structural analysis of fluoride-phosphate and fluoro-phosphate glasses. J Non-Crystalline Solids X. 2019;3:100026.
32. Diwakar PK, Loper KH, Matiaske A-M, Hahn DW. Laser-induced breakdown spectroscopy for analysis of micro and nanoparticles. J Anal Atom Spectrom. 2012;27(7):1110–9.
33. Foucaud Y, Fabre C, Demeusy B, Filippova IV, Filippov LO. Optimisation of fast quantification of fluorine content using handheld laser induced breakdown spectroscopy. Spectrochim Acta B-Atomic Spectroscopy. 2019;158:105628.
34. Legnaioli S, Campanella B, Poggialini F, Pagnotta S, Harith MA, Abdel-Salam ZA, et al. Industrial applications of laser-induced breakdown spectroscopy: a review. Anal Methods. 2020;12(8):1014–29.
35. Windom BC, Hahn DW. Laser ablation—laser induced breakdown spectroscopy (LA-LIBS): a means for overcoming matrix effects leading to improved analyte response. J Anal Atom Spectrom. 2009;24(12):1665–75.
36. Hahn DW, Omenetto N. Laser-induced breakdown spectroscopy (LIBS), Part II: review of instrumental and methodological approaches to material analysis and applications to different fields. Appl Spectros. 2012;66(4):347–419.
37. De Lucia FC, Gottfried JL. Rapid analysis of energetic and geo-materials using LIBS. Mat Today. 2011;14(6):274–81.
38. González R, Lucena P, Tobaria LM, Laserna JJ. Standoff LIBS detection of explosive residues behind a barrier. J Anal At Spectrom. 2009;24(8):1123–6.
39. Alvarez-Llamas C, Pisonero J, Bordel N. A novel approach for quantitative LIBS fluorine analysis using CaF emission in calcium-free samples. J Anal Atom Spectrom. 2017;32(1):162–6.

40. Negre E, Motto-Ros V, Pelascini F, Lauper S, Denis D, Yu J. On the performance of laser-induced breakdown spectroscopy for quantitative analysis of minor and trace elements in glass. J Anal Atom Spectrom. 2015;30(2):417–25.
41. Quarles CD, Gonzalez JJ, East LJ, Yoo JH, Morey M, Russo RE. Fluorine analysis using Laser Induced Breakdown Spectroscopy (LIBS). J Anal At Spectrom. 2014;29(7):1238–42.
42. Hill RG, Brauer DS. Predicting the bioactivity of glasses using the network connectivity or split network models. J Non-Cryst Solids. 2011;357(24):3884–7.
43. Eden M, Sundberg P, Stalhandske C. The split network analysis for exploring composition-structure correlations in multi-component glasses: II. Multinuclear NMR studies of alumino-borosilicates and glass-wool fibers. J Non-Cryst Solids. 2011;357(6–7):1587–94.
44. Hill R. An alternative view of the degradation of bioglass. J Mater Sci Lett. 1996;15(13):1122–5.
45. Peitl O, Dutra Zanotto E, Hench LL. Highly bioactive P_2O_5–Na_2O–CaO–SiO_2 glass-ceramics. J Non-Cryst Solids. 2001;292(1):115–26.
46. Brauer DS, Karpukhina N, Law RV, Hill RG. Structure of fluoride-containing bioactive glasses. J Mater Chem. 2009;19(31):5629–36.
47. Pedone A, Charpentier T, Menziani MC. The structure of fluoride-containing bioactive glasses: new insights from first-principles calculations and solid state NMR spectroscopy. J Mater Chem. 2012;22(25):12599–608.
48. Pouzar M, Kratochvíl T, Kaski S, Kaiser J, Knotek P, Čapek L, et al. Effect of particle size distribution in laser-induced breakdown spectroscopy analysis of mesoporous V-SiO2 catalysts. J Anal At Spectrom. 2011;26(11):2281–8.
49. Xu XJ, Day DE, Brow RK, Callahan PM. Structure of tin fluorophosphate glasses containing PbO or B_2O_3. Phys Chem Glasses. 1995;36(6):264–71.
50. Gonçalves TS, Moreira Silva RJ, de Oliveira Junior M, Ferrari CR, Poirier GY, Eckert H, et al. Structure-property relations in new fluorophosphate glasses singly- and co-doped with Er^{3+} and Yb^{3+}. Mater Chem Phys. 2015;157:45–55.
51. de Oliveira M, Gonçalves TS, Ferrari C, Magon CJ, Pizani PS, de Camargo ASS, et al. Structure-property relations in fluorophosphate glasses: an integrated spectroscopic strategy. J Phys Chem C. 2017;121(5):2968–86.
52. Ehrt D. REVIEW: Phosphate and fluoride phosphate optical glasses properties, structure and applications. Phys Chem Glasses Eur J Glass Sci Technol Part B. 2015;56(6):217–34.
53. Semrau KT. Emission of Fluorides from industrial processes—a review. JAPCA J Air Waste Ma. 1957;7(2):92–108.
54. Christie JK, Pedone A, Menziani MC, Tilocca A. Fluorine environment in bioactive glasses: ab Initio molecular dynamics simulations. J Phys Chem B. 2011;115(9):2038–45.
55. Hill R, Wood D, Thomas M. Trimethylsilylation analysis of the silicate structure of fluoro-alumino-silicate glasses and the structural role of fluorine. J Mater Sci. 1999;34(8):1767–74.
56. Djouama T, Boutarfaia A, Poulain M. Fluorophosphate glasses containing manganese. J Phys Chem Solids. 2008;69(11):2756–63.
57. Parsons AJ, Sharmin N, Shaharuddin SIS, Marshall M. Viscosity profiles of phosphate glasses through combined quasi-static and bob-in-cup methods. J Non-Cryst Solids. 2015;408:76–86.
58. Döhler F, Groh D, Chiba S, Bierlich J, Kobelke J, Brauer DS. Bioactive glasses with improved processing. Part 2. Viscosity and fibre drawing. J Non-Cryst Solids. 2016;432:130–6.

SUPPORTING INFORMATION

Additional supporting information may be found online in the Supporting Information section.

How to cite this article: Pablos-Martín A, Contreras Jaimes AT, Wahl S, Meyer S, Brauer DS. Fluorine loss determination in bioactive glasses by laser-induced breakdown spectroscopy (LIBS). *Int J Appl Glass Sci*. 2021;00:1–9. https://doi.org/10.1111/ijag.15867